Circadian genes in a blind subterranean mammal II: Conservation and uniqueness of the three *Period* homologs in the blind subterranean mole rat, *Spalax ehrenbergi* superspecies

Aaron Avivi*[†‡], Henrik Oster[†§¶], Alma Joel*, Avigdor Beiles*, Urs Albrecht[§¶], and Eviatar Nevo*

*Laboratory of Animal Molecular Evolution, Institute of Evolution, University of Haifa, Mount Carmel, Haifa 31905, Israel; [§]Max-Planck-Institute for Experimental Endocrinology, Feodor-Lynen-Strasse 7, 30625 Hannover, Germany; and [¶]Department of Medicine, Division of Biochemistry, University of Fribourg, Rue du Musée 5, 1700 Fribourg, Switzerland

Contributed by Eviatar Nevo, July 10, 2002

We demonstrated that a subterranean, visually blind mammal has a functional set of three *Per* genes that are important components of the circadian clockwork in mammals. The mole rat superspecies *Spalax ehrenbergi* is a blind subterranean animal that lives its entire life underground in darkness. It has degenerated eyes, but the retina and highly hypertrophic harderian gland are involved in photoperiodic perception. All three *Per* genes oscillate with a periodicity of 24 h in the suprachiasmatic nuclei, eye, and harderian gland and are expressed in peripheral organs. This oscillation is maintained under constant conditions. The light inducibility of *sPer1* and *sPer2*, which are similar in structure to those of other mammals, indicates the role of these genes in clock resetting. However, *sPer3* is unique in mammals and has two truncated isoforms, and its expressional analysis leaves its function unresolved. *Per*'s expression analysis in the harderian gland suggests an important participation of this organ in the stabilization and resetting mechanism of the central pacemaker in the suprachiasmatic nuclei and in unique adaptation to life underground.

Life on Earth is adapted to cyclical phenomena imposed by the external environment (1). Most organisms have circadian systems that synchronize physiological events to the external 24-h cycle (2). The underlying molecular-genetic mechanisms of these clocks exhibit an extraordinary evolutionary conservation from cyanobacteria through plants, fruit flies, and mammals. All of these clock systems consist of autoregulatory transcriptional/translational feedback loops with positive/negative regulatory elements and similar genetic machinery (3, 4).

Two basic helix–loop–helix PAS (PER-ARNT-SIM) transcription factors, CLOCK and MOP3 (BMAL1), form the positive elements of the system and drive transcription of three *Period* (*Per 1, 2, 3*) and two *Cryptochrome* (*Cry 1, 2*) genes. The protein products of these genes are thought to be components of a negative feedback complex that inhibits the CLOCK/MOP3 heterodimer, thereby closing the circadian loop.

The enigma of circadian rhythms in a blind subterranean mammal is intriguing (5–7). We have already shown that a CLOCK/MOP3-driven clock exists in *Spalax* (8). Here we continue to decipher its circadian machinery.

The Evolutionary Model of Blind Subterranean Mammals

The blind subterranean mammals, mole rats of the *Spalax ehrenbergi* superspecies in Israel, consist of four species that have been studied multidisciplinarily as an evolutionary model of speciation and adaptation (5–7). *Spalax* lives in total darkness, yet, it perceives the daily and seasonal temporal cycles underground (9). Behaviorally, *Spalax* displays polyphasic and polytypic day-night activity patterns (10, 11) coupled with polymorphic (12) and seasonal[‖] variation, supported by a unique photoperiodic perception mechanism (9). *Spalax* has a degenerated s.c. functional eye (13, 14), which, together with the harderian gland, participates in photoperiodic perception (9, 15–18). The retina harbors *Rhodopsin* (19, 20) and *Coneopsin* (21), adaptively effective in photoperiodic perception (22, 23), and expresses *alfa-B-crystallin* (24). The photic signals entrain *c-fos* in the suprachiasmatic nuclei (SCN) Zeitgeber (25) and can possibly activate circadian genes.

Evolutionarily, *Spalax*'s perceptive brain structures (SCN and striatum) were expanded and sight pathways were drastically (>90%) reduced. The visual cortex was replaced by somatosensory cortex (26–28), *Per* homologous ACNGGN-repeats cycle in the hypothalamus (29) and melatonin precursors occur in the harderian and pineal glands and retina (30).

What is the genetic basis of circadian rhythmicity in *Spalax*? We cloned, sequenced, and unraveled the expression of the circadian *Clock* and *MOP3* cDNAs of three species of the *S. ehrenbergi* superspecies in Israel (8). Both genes are relatively conserved, yet *Clock* displays a unique Q-rich area as compared with other mammals, assumed to function in circadian rhythmicity, and *Spalax* CLOCK/MOP3 dimer is less potent than its human counterpart in driving transcription.

Here we describe the cloning, sequencing, and expression of the three *Period* cDNAs of *Spalax*. Its three *Per* cDNAs are conserved, yet they show features unique to *Spalax* especially in *Per3*, *Per1*, and *Per2* cycles in the SCN, eye, and harderian gland. *Per3* is structurally unique among studied sighted mammals and awaits functional elucidation.

Materials and Methods

Animals. We analyzed adults (100–150 g), belonging to *Spalax judaei*, ($2n = 60$) from Anza, Samaria (7). Field-trapped animals were kept at 22–24°C with seasonal photoperiod. We selected diurnal animals that were kept under a 12-h light/12-h dark cycle. For analysis of *Per* transcriptional activity in constant darkness, light was turned off at Zeitgeber time (ZT) 12, and animals were kept in the dark for at least 2 days before being killed under dim illumination (15-W safety red light). Light inducibility experiments were done on animals kept in light/dark for a week with a short light pulse (15 min, >200 Lx) at specified ZT followed by release into constant darkness. For gene induction analysis brains were taken 1 h after illumination. Each experiment was done on three sets of animals.

Abbreviations: SCN, suprachiasmatic nuclei; ZT, Zeitgeber time; RT-PCR, reverse transcription–PCR; ISH, *in situ* hybridization; CK1ε, casein kinase 1ε.

Data deposition: The sequences reported in this paper have been deposited in the GenBank database (accession nos. AJ345059–AJ345062).

[†]A.A. and H.O. contributed equally to this work.

[‡]To whom reprint requests should be addressed. E-mail: aaron@esti.haifa.ac.il.

[‖]Kushnirov, D., Beolchini, F., Lombardini, F. & Nevo, E., Euro-American Mammal Congress, July 24–28, 1998, Santiago de Compostela, Spain, p. 381.

Cloning of *Spalax Per* cDNAs. We cloned the three *Spalax Per* cDNAs by reverse transcription–PCR (RT-PCR) (31). Oligos were synthesized according to the ORF of the known human and mouse homologous sequences (GenBank accession nos. AF022991, AB002370, and AB047686 for human *Per1, Per2*, and *Per3*, respectively and AF022992, AF036893, and AB013605 for mouse *Per1, Per2*, and *Per3*, respectively). Whole brain total RNA was prepared by using the TriReagent RNA isolation reagent (Molecular Research Center, Cincinnati). First-strand cDNA was synthesized with oligo(dT) as a primer and Super-Script II reverse transcriptase enzyme (GIBCO/BRL). This cDNA product was taken for PCR by using *Taq*DNA polymerase (Appligene, Strasbourg, France). The annealing temperature, elongation time, and $MgCl_2$ concentration were adjusted for each specific PCR. In the case of *sPer3* isolation, we verified our RT-PCR results by also cloning through cDNA library screening (32). *Spalax* brain cDNA library in Lambda-TripleEx was screened by using a partial *mPer3* cDNA as a probe. Sequencing was determined by thermocycling sequencing using di-deoxy nucleotide terminators (3700 DNA Analyzer, Perkin–Elmer/Applied Biosystems) at the sequencing unit of the Weizmann Institute of Science (Rehovot, Israel).

Evolutionary Analysis. The evolutionary analysis of the *Per* cDNAs presented here is based on distances and divergence calculations (Wisconsin package version 10, GCG).

The DISTANCES program (33) calculates pairwise distances between aligned sequences expressed as substitutions per 100 bases or amino acids. To correct the distances for multiple substitutions at a site, we used Kimura's nucleic acid (33) and protein (34) methods.

The DIVERGE program estimates the pairwise number of synonymous and nonsynonymous substitutions per site between two or more coding aligned nucleic acid sequences (35, 36).

***In Situ* Hybridization (ISH).** Tissues used for ISH were treated and examined as described in Albrecht *et al.* (37). The *Spalax Per1* probe corresponded to nucleotides 615-1300, the *sPer2* probe corresponded to nucleotides 85–605, and the probe of *sPer3* corresponded to nucleotides 1751–2590.

Quantification was performed by densitometric analysis of hybridization signals on x-ray films with Scion (Frederick, MD) IMAGE 4.0.2 software. For silver grain images, tissue was visualized by fluorescence of Hoechst dye-stained nuclei, and silver grain signals were artificially colored for clarity. Quantitation of ISH results was analyzed with GraphPad (San Diego) PRISM software. Data sets were compared by ANOVA with subsequent Bonferroni correction for multiple comparisons, with $P < 0.05$ as the criterion of significance.

Quantitative RT-PCR. For quantitation of the *sPer* genes expression in the harderian gland and the liver of *Spalax*, a quantitative RT-PCR was performed. Equal amounts of total RNA from animals killed at the relevant ZT points were taken for first-strand cDNA synthesis (see above). The cDNAs were synthesized by adding equal traces of [^{32}P]dCTP to ensure equal amounts of cDNA templates in the PCRs. For the PCR we used oligos synthesized according to the sequence of the different *sPer* isolated clones. For each *Per* gene quantitation we used one sense 5′ oligo and two antisense 3′ oligos (3′[1] and 3′[2]), giving rise to two distinct products (450–600 bp). One set of oligos (5′ and 3′[1]) was used for the harderian gland and the other (oligos 5′ and 3′[2]) for the liver, in the same PCR tube. A second PCR was carried out by changing the 3′ oligo between the harderian and liver tissues. In each PCR, a 300-bp fragment of actin, as an internal control, was also synthesized, using specific actin oligos. Each cDNA was first tested for different PCR amplification cycles with the different sets of oligos. The final experimental PCRs were performed at the logarithmic phase of the reaction for each specific cDNA of interest (18–22 cycles). Each experiment was carried out on two RNA samples taken from two different individuals, and each PCR was repeated three times. The PCR products were then run on ethidium bromide/1.3% agarose gels. The gels were subjected to quantitation of the specific bands by the Eagle Eye II system (Stratagene). The system integrates the density of the ethidium bromide of a rectangle limiting a specific band in pixel values. The values received for the specific *Per* bands were normalized according to the values received for the actin bands (which were statistically equal in the different tissues and in the different reactions).

Results

Cloning and Structural Analysis of the Three *Spalax Per* (*sPer*) Genes. Analysis of the ORFs of *Spalax Per* cDNAs revealed transcripts of 1,062 aa residues for *sPER1* (GenBank accession no. AJ345059) and 1,248 aa for *sPER2* (GenBank accession no. AJ345060). For *sPER3* we isolated two truncated deduced proteins, one with 489 aa (isoform a, GenBank accession no. AJ345061) and the other with 583 aa (isoform b, GenBank accession no. AJ345062). Identified functional domains like the PAS domain and the basic helix–loop–helix motif are highly similar in sPER1 and sPER2, but the homology in sPER3 is low. The recently identified casein kinase 1ε (CK1ε) binding site of human PER2 and the five putative phosphorylation sites (AA 668, 671, 674, 677, and 680) (38) are conserved in PER proteins of *Spalax*, mice, and humans with the exception of sPER3. Hence sPER3 is probably not a substrate for the *Spalax* CK1ε ortholog.

Evolutionary Analysis of the *Spalax Per* Genes. Protein trees of PER1, PER2, and PER3 in *Spalax*, mice, rats, and humans appear in Fig. 1. The *Drosophila* Per (GenBank accession no. X03636) was also compared, but it was very different from the three mammalian Per proteins. The computer program used (GCG10) estimated the distance of the dPer from its mammalian counterparts as maximal and beyond the accuracy of the method.

The estimated divergence time between *Spalax* and other rodents is much shorter than the divergence between humans and rodents. Therefore, we expected that the genetic distance between *Spalax* and mice or rats would be considerably smaller than between humans and these two rodents. We also expected that the distance between humans and *Spalax* and between humans and mice or rats would be similar. Any divergence from these expectations can suggest that additional factor(s) influence the rate of evolution of the *Per* genes of *Spalax* and, therefore, deviate from the phylogenetic divergence time.

Below we present the evolutionary analysis for each *Per* gene separately.

Per1. There is agreement between the above evolutionary expectations and the PER1 proteins (Fig. 1 *Top*) and *Per1* nucleotide sequence (tree not shown). The relative distances in protein and nucleotides between *Spalax* and mice are 75% (6.85 vs. 9.12) and 80% (10.51 vs. 13.18) of the distances between *Spalax* and humans, respectively. The distances between rodents (*Spalax* and mice) and humans are similar: 9.12 and 8.04 in the protein and 13.18 and 13.26 in the nucleotide sequence.

Per2. Rat PER2 (GenBank accession no. MN031678) was also included and expected to be similar to mouse PER2. As in Per1, PER2 results were in agreement with the phylogenetic expectations (Fig. 1 *Middle*). The relative distances between *Spalax* and mice were 42% (11.55 vs. 27.54) or 59% (13.07 vs. 22.09) of the distances between *Spalax* and humans in protein and nucleotides, respectively. The distances between *Spalax* and rats were 46% (12.69 vs. 27.54) or 66% (14.6 vs. 22.09) of the distances between *Spalax* and humans in protein and nucleotides, respectively. The distances between rodents (mice, rats, and *Spalax*)

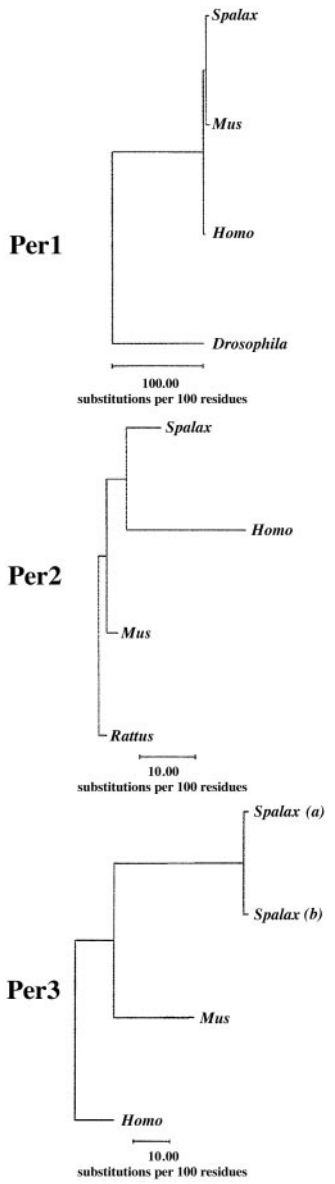

Fig. 1. Similarity tree of the three Per-deduced proteins. The unrooted tree depicts the similarity relationships of the three PER proteins (amino acids) in *Spalax*, mice, rats, humans, and *Drosophila*.

and humans were also similar: 27.00, 27.70, and 27.54 for protein and 22.56, 23.58, and 22.09 for nucleotides, respectively.

Per3. As mentioned, we cloned two truncated clones of *Spalax Per3* (named a and b). Both clones start at the equivalent of mouse 468 bp (110 bp 3′ to the mouse ATG initiation codon). We could not isolate any further 5′ sequences either through RT-PCR or cDNA library screening. Both clones contain an insertion of 198 bp at position 1211 bp of mice that interrupts the ORF. Furthermore, *sPer3*a has two deletions, the prominent one is 432 bp in length starting at position 1478 bp of the mouse sequence. At the starting point of this deletion in *sPer3*a, *sPer3b* has a cluster of termination codons at any of the three reading frames. The apparent initiation ATG is located immediately after the deletion in the *sPer3*a or these termination codons in *sPer3b*. Omitting the changes in the *sPer3b* clone yielded a *Spalax Per3* ORF, which is similar to that of mice and humans. It should be emphasized that similar products have never been obtained in negative control amplifications with templates generated

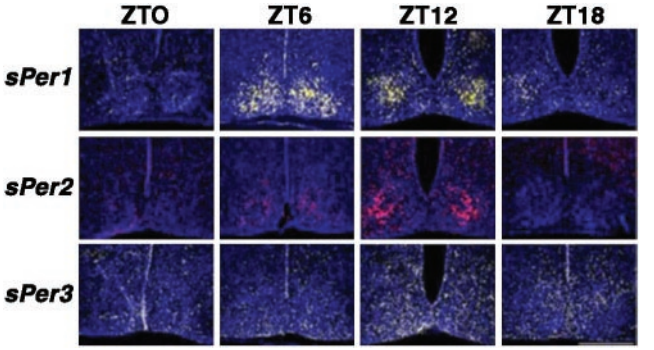

Fig. 2. Diurnal expression of *sPer1*, *sPer2*, and *sPer3* of *Spalax* in the SCN: coronal sections through the brain. Blue color represents Hoechst-stained nuclei. (*Top*) The yellow signal shows the expression of *Spalax Per1* over 24 h measured at 6-h time intervals (ZT0: lights on; ZT12: lights off). Maximal expression is seen at ZT6. (*Middle*) The red signal shows the expression of *sPer2* in representative sections. Maximal expression is seen at ZT12. (*Bottom*) The green signal shows the expression of *sPer3* in representative sections. Maximal expression is at ZT12. Note that *sPer1* and *sPer2* expression is mainly in the SCN, whereas *sPer3* expression is weaker and spreads in different areas of the brain. (Magnification: ×20.)

without reverse transcriptase enzyme, eliminating the possibility of genomic DNA contamination. Furthermore, the *sPer3* clones that were isolated from the *Spalax* brain cDNA library contain a shorter 3′ untranslated region than those of mice and humans, and in contrast to them, contain an adenylation site 940 bp 3′ to the termination TAA codon. The published 3′ untranslated regions of mice (1,164 bp) and humans (2,421 bp) do not reach the adenylation site. Southern blot analyses suggest that the *Spalax sPer3* is probably a pseudogene (results not shown).

The nucleotide distances between *Spalax Per3* and that of mice or humans are similar. The protein distances (Fig. 1 *Bottom*) between the two *Spalax* PER3 and mice or humans were 56.21 vs. 57.20 for sPER3a, respectively and 60.41 vs. 57.74 for sPER3b, respectively. Kimura's two-parameter nucleotide distance analysis (33) gave more than two substitutions per bp. Thus, the exact calculated value is meaningless and depends heavily on the assumptions of the correction factors. Nevertheless, the calculated distance of *Spalax* vs. mice is even larger than the calculated distance of *Spalax* vs. humans. The same is true for the distances calculated separately for synonymous and nonsynonymous substitutions.

Synonymous vs. Nonsynonymous Substitutions in the *Per* Family. Our calculations show that *Per2* has a ratio around 0.2, indicating that it attained optimum function before the divergence of the species. *Per1* and *Per3* have a ratio of 0.43 to 0.75, a relatively high ratio suggesting adaptive evolution. The *Drosophila Per* showed a ratio >1.0, indicating positive selection for a functional change.

***sPer* Genes Oscillate in the *Spalax* SCN.** ISH with antisense riboprobes in the brain revealed a rhythmic pattern of expression for s*Per1* and s*Per2*, mainly in the SCN but *sPer3* is widely spread in the brain (Fig. 2). Maximal expression for s*Per1* was at ZT6 and for s*Per2* and s*Per3* at ZT12. The amplitude of *sPer3* expression was markedly lower ($P < 0.05$) than that of s*Per1* and s*Per2.* The sense (control) riboprobes of the three *sPer* had a reproducible background hybridization that did not overlap with the antisense probe. No rhythmic expression with the sense riboprobe hybridization intensity was noted.

***sPer* Genes Exhibit a Diurnal Oscillation in *Spalax* Peripheral Tissues.** Significant expression of the three *sPer* genes was noted, using RT-PCR, in lung, intestine, liver, harderian gland, eye, brain, and skeletal muscle (data not shown).

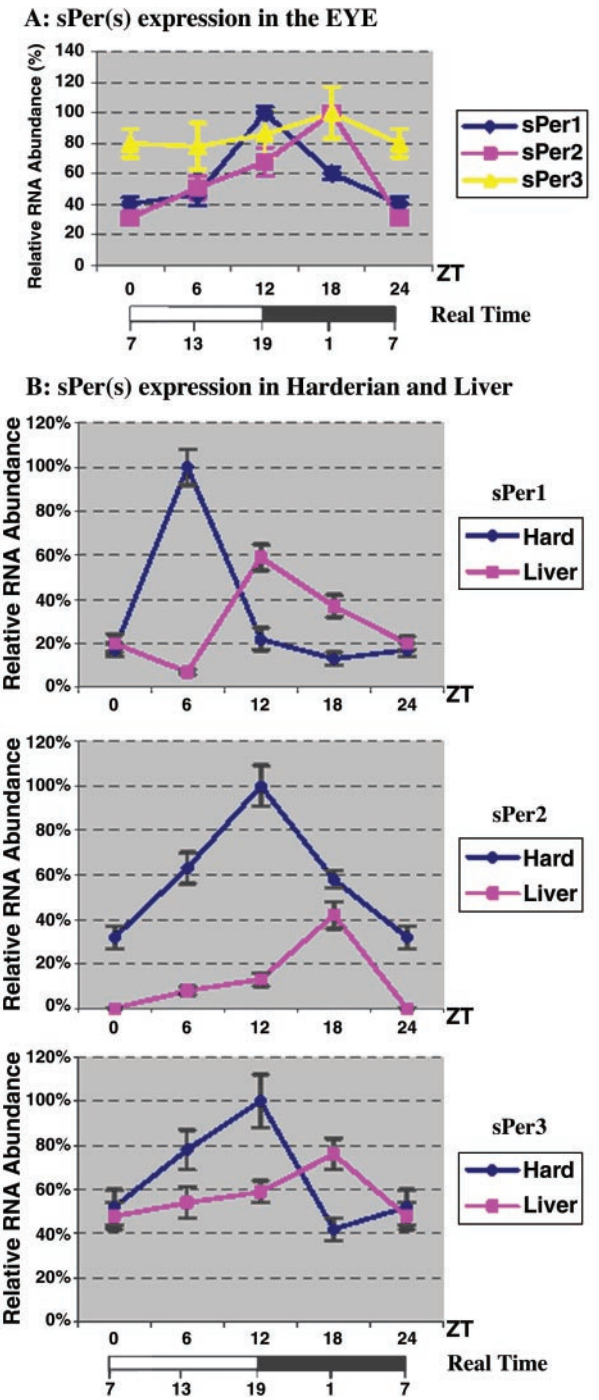

Fig. 3. Expression of *Spalax Per* genes in peripheral tissues. (*A*) Densitometric analysis of silver grain *in situ* staining in the eye. The maximal expression in the eye shows that the expression of the three *sPer* genes is shifted by 6 h as compared with their expression in the SCN (Fig. 2). The oscillation of *sPer3* is very weak ($P > 0.05$). (*B*) Expression of the three *sPER* genes in the harderian gland and liver quantitated by RT-PCR. The expression peaks of all three *sPer* genes in the harderian gland are synchronized with the SCN (see Fig. 2), whereas the peak of expression in the liver is shifted by 6 h. As in the SCN, the difference in *sPer3* expression in ZT6 and ZT12 is very small ($P > 0.05$).

The *Spalax* Eye. In the *Spalax* eye (Fig. 3*A*) ISH revealed a shift of 6 h in the expression maxima of all three *Per* genes compared with the expression in the SCN. Expression of s*Per1* was maximal at ZT12 and of s*Per2* and *sPer3* at ZT18, but for *sPer3*, the amplitude of expression was very small. Thus the RNA rhythms for all three *Per* genes of *Spalax* are present in the photoperiodic retina, the site of light detection.

The *Spalax* Harderian Gland. Expression maxima in the harderian gland could be observed by quantitative RT-PCR (Fig. 3*B*) and ISH (data not shown) at the following ZTs: s*Per1* at ZT6 and s*Per2* and s*Per3* at ZT12. Quantitative RT-PCR analysis in the liver (Fig. 3*B*) revealed rhythmic expression of s*Per* genes with maxima of *sPer1* at ZT12 and of *sPer2* and *sPer3* at ZT18. The oscillation in the *Spalax* liver, as in its eye, shows a 6-h delay compared with the *Spalax* SCN. However, the circadian rhythm in the *Spalax* harderian gland is synchronous with the expression pattern in the *Spalax* SCN.

The Circadian Oscillation of *sPer* Genes Is Maintained in Constant Darkness. *sPer* gene RNA levels in the SCN, eye, and harderian gland were studied at four time points over a 24-h period, on the second day in constant darkness (not shown). ISH revealed that RNA levels of all three *sPer* genes were rhythmic and the oscillation pattern under constant darkness was similar to that under 12-h light/12-h dark conditions. Highest levels were observed during the subjective day in the SCN at circadian time 6 for *sPer1* and circadian time 12 for *sPer2* and *sPer3*. The peak levels of mRNA in the eye were 6 h later than in the SCN, but were synchronized with the SCN in the harderian gland. The amplitude of *sPer3* rhythmicity was markedly lower than that of *sPer1* and *sPer2* in all three tissues studied and only nearly significant ($P > 0.05$).

Differential Light Regulation of *Spalax Per* Genes. Previous studies have shown that *mPer1* and *mPer2* expression in the SCN is induced by exposure to light at night (39, 40), whereas *mPer3* is unaffected (41). We examined inducibility of the s*Per* genes in the SCN, eye, and harderian gland by nocturnal light pulses at ZT14 and ZT22 (Fig. 4). These time points were chosen for study as light pulses at these times produce phase delays and advances in locomotor activity.

Quantitation of the *in situ* results showed that 1 h after a light pulse at ZT14, *sPer1* and *sPer2* were significantly induced in all three tissues. Remarkably, the level of *sPer1* induction in the harderian gland was significantly ($P < 0.05$) higher than in the SCN or the eye, reinforcing its great importance for the *Spalax* clock. One hour after the light pulse at ZT22 only *sPer1* was significantly induced in the three tissues examined. Like the *sClock* gene, s*Per3* gene was not light inducible either at ZT14 or ZT22 in the three tissues tested.

Discussion

Adaptive Selection on *Per* Genes in *Spalax* to Life Underground in Total Darkness. Like other mammals, the subterranean blind *Spalax* has three *Per* genes.

The distances between *sPer1* and *sPer2* and those of other rodents or humans are as expected from their divergence time, which is estimated to be 40 million years ago and 80 million years ago, respectively (6). The distances between *Spalax* or mice and humans are similar, as expected. Generally, the distances calculated for *Per2* are larger than the distances for *Per1*. In our analysis of synonymous vs. nonsynonymous substitutions we relied on Liberles *et al.* (42), who suggested using this ratio to reveal selection for change in enzymatic function. Data of Makalowski and Boguski (43) show that most rodents and human sequences have a ratio of 0.2. This finding indicates that such proteins, selected over millions of years, attained an optimum function before the divergence of rodents and primates and subsequent evolution was relatively conservative. They also considered ratios between 0.6 and 1.0 as suggesting a relaxation of functional constraint and selection. Our results show that *sPer1* and *sPer3* have a ratio of 0.4 to 0.6 and *sPer2* has a ratio of about 0.2. Hence, presumably, *sPer2* has not been changed to

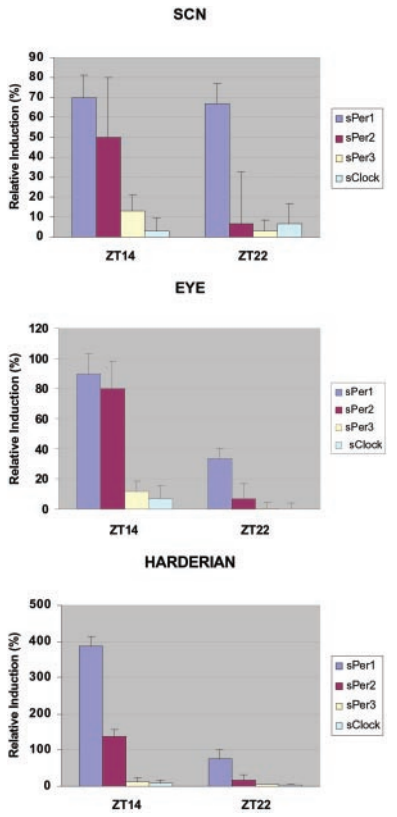

Fig. 4. Light inducibility of the three *Spalax Per* genes' expression. Animals were given a 15-min light pulse at ZT14 and ZT22 and killed 1 h later. Coronal sections through the brain and ISH were performed on treated (ZT14 pulse and ZT22 pulse) and control animals that were killed at the same time. Relative mRNA induction was analyzed by densitometric analysis of *in situ* silver grain staining. *sClock* inducibility is given as negative control. (*Top*) In the SCN, *sPer1* is equally inducible at ZT14 and ZT22. *sPer2* is inducible only at ZT14, whereas *sPer3* gene shows no measurable changes in expression levels at the two time points. (*Middle*) Inducibility of *sPer1*, *sPer2*, and *sPer3* in the eye is similar to that in the SCN. (*Lower*) In the harderian gland, *sPer1* is highly inducible at ZT14 and less at ZT22 whereas *sPer2* expression is light sensitive only at ZT14. *sPer3* shows no light inducibility at either time point. Note the significantly ($P < 0.01$) higher induction of *sPer1* in the harderian gland compared with the other tissues after light pulse at ZT14. Note the different *y*-axis scales in SCN, eye, and harderian.

function in a visually blind mammal living in a dark environment with negligible light cues. However, the figures obtained for *sPer1* and *sPer3* may suggest that molecular changes in these genes were necessary to fulfill their expected adaptive function in darkness. If we combine the calculated distances and the high ratio of nonsynonymous substitutions, the result supports the hypothesis of adaptive changes caused by natural selection, possibly in response to life in darkness underground.

sPer3 evinces a different situation. First, this locus in *Spalax* underwent major changes of deletions and insertions, resulting in two isoforms exhibiting truncated coding regions; somewhat similar results were reported for the *hPer4* pseudogene (44). However, *sPer3* is very different from *hPer4*. Its insertion could not be identified with any known sequence, in contrast to the fossil MER-2 mobile element that is within the *hPer4* locus (44). When the changes in the *sPer3* are omitted, an ORF similar to *mPer3* is obtained. When the distances were calculated from the aligned shortened sequences the phylogenetic expectations were not met. The distances between *sPer3* and *mPer3* are similar or even larger than the distances between *sPer3* and *hPer3*. This finding may support adaptive selective changes in the evolution of this gene and not just the neutral accumulation of substitutions over time. The comparison of *sPer3* expression patterns with *sPer1* and *sPer2*, which was described here and is discussed below, raises questions as to the role that *sPer3* plays in the *Spalax* circadian system.

The Functional Circadian Domains of *Spalax Per* Genes. *sPer1* and *sPer2* contain all functionally relevant domains discovered in other mammalian PER proteins so far. The basic helix–loop–helix motif as well as the PAS domain consisting of PAS A, PAS B (39, 45), and PAC CK1ε binding and phosphorylation sites (38) are conserved, suggesting their role as a CK1ε substrate in the central mechanism of the *Spalax* circadian clockwork. Remarkably, the whole putative CK1ε binding site as well as the N-terminal basic helix–loop–helix motif are missing in *sPer3*. This finding supports a speculation about its role in the biological clock (45).

Because *Spalax* is visually blind and lives entirely underground, hence denied outside Zeitgeber information (6), a robust and precise internal clock is necessary for the animal to keep track of time under negligible light cues. Indeed, *in situ* data revealed that *Spalax Per* genes' expression is clearly rhythmic and maintained under constant conditions and in constant darkness. *sPer1* and *sPer2* expression in the *Spalax* brain is concentrated mainly in the SCN. However *sPer3* is widely spread in different areas of the brain, similar to what has been reported for the mouse *Per3* (41), and its oscillation levels are less prominent than those of *sPer1* and *sPer2*. These findings raise a question as to the role of *Per3* in the circadian system. The central pacemaker of the SCN signals time to the retina and peripheral clocks, as in the liver, where the circadian genes' expression follows its rhythm with a delay of 4–6 h (41, 46). The blind *Spalax Per* genes' expression is similar, and our results also show a lag of 6 h in the peak expression of the *Per* genes in the retina and liver. Although the exact role of *Spalax Per3* in the maintenance of the circadian rhythm remains unresolved, it may prove substantial for time keeping underground.

The Harderian Gland: A Circadian Center in *Spalax*. Noteworthy, mRNA levels in the *Spalax* hypertrophic harderian gland oscillate synchronously with the SCN. Similar synchronization in the peak levels of mRNA in the SCN and the harderian gland was seen also for *Spalax MOP3* gene (8), the dimerization partner of the CLOCK protein (47) and an essential component of the circadian pacemaker in mammals (48). Furthermore, *sPer1* inducibility in the harderian gland after light pulse during the dark phase of the clock cycle is much higher than in the SCN. The harderian gland of *Spalax* is extraordinarily enlarged and occupies the entire eye socket, presumably as an adaptation to life underground. Previous studies (15) suggested that the harderian gland of *Spalax* is a possible photoreceptor and photoperiodic organ. Given its exposed position directly behind the atrophied minute eye, it seems likely that the harderian gland has a prominent role in the *Spalax* clock mechanism. This gland may demonstrate the extreme of evolutionary progression during the adaptive morphological and molecular reorganization for life underground (6).

Differential Regulation of *Spalax Per* Genes. Light inducible experiments in *Spalax* reveal that *sPer1* is light inducible both early (ZT14) and late (ZT22) at night, whereas *sPer2* is light inducible only at the beginning of the night. This result is in accordance with the findings of Albrecht *et al.* (39). *sPer3* levels are unresponsive to light pulses applied throughout the dark phase of the circadian cycle. This differential regulation among the three *sPer* genes suggests that each has a different regulatory function in the SCN. The behavioral effects of photic stimuli at these two time points (ZT14 and ZT22) have been characterized in mice (49, 50). Light pulse at ZT14 causes phase delays in behavioral rhythms and light pulse at ZT22 causes phase advances. Our results indicate a role of *sPer1* in both phases and of *sPer2* in the phase-delay mechanism. Our *in situ* data provide a molecular confirmation of previous

behavioral studies in *Spalax* (11) and link the activity pattern of these species with the cellular cycling in sighted animals. The poor *sPer3* oscillation and the absence of light influence on *sPer3* expression levels may suggest a role for *sPer3* outside the central pacemaker. This finding is consistent with data from *Per3*-deficient mice (51, 52) but may prove an adaptation to life underground and deserves further critical studies.

All three *Spalax Per* genes are expressed in a wide variety of nonneural tissues as previously shown in *Drosophila* (53, 54) and mice (39, 41). In three of these tissues (liver, eye, and harderian gland) we found that the RNA levels for the three *sPer* genes oscillate. Oscillation of *sPer* genes in the eye, the target organ of light absorption, is rational. As we already suggested, the oscillation of the *sPer* genes in the *Spalax* harderian gland is in accordance with previous results, suggesting an important role of this tissue in circadian maintenance (15) and merits further intensive study. The oscillation in the liver and the widespread expression in other peripheral tissues that were examined suggest the existence of clocks outside the SCN.

Molecular-Genetic Tinkering of Circadian Genes in a Blind Mammal. This study substantiates the claim that the blind subterranean *Spalax* needs a photoperiodic system to perceive daily and seasonal cycles. It has retained a functional retina with effective visual pigment genes signaling to the SCN (14, 17–20, 23, 24) presumably induced by the small amount of photons that penetrate underground to an otherwise dark environment. Circadian genes in the retina, harderian gland, SCN, and other tissues, including *Clock* (8) and the three *Per* genes described here, process the light signals and translate them into the unique behavioral repertoire of *Spalax*, including polyphasic, polymorphic, and seasonal behavioral phenotypes. In this respect we should emphasize that *Spalax* exhibits naturally occurring predominantly either diurnal or nocturnal individuals. Currently we are studying the expression pattern of the *Per* genes in naturally occurring nocturnal animals or on diurnal animals after a phase shift of light. The mosaic evolution of the *Spalax* eye (17, 18), harderian gland (30), and brain (26–28) and its circadian genes provide a striking model of tinkering evolution at both the molecular and organismal levels. From an evolutionary perspective the genetic basis of circadian rhythms in the blind subterranean *Spalax* may be different from that of strictly diurnal or nocturnal and sighted mammals. Identification of the circadian genes of blind *Spalax* might advance insights into the structure and evolution of the circadian organization in mammals, including humans, at the molecular level and their ecological causation. Remarkably, the colonization of the subterranean dark ecological zone by *Spalax* did not obliterate the conservative circadian rhythmicity and its genetic basis of photoreceptiveness and clock genes. All of the circadian machinery was adaptively transformed to perceive light in darkness.

We thank Dr. Z. S. Sun for his initial help with the cloning of the *Spalax Per1* probe. We are also grateful to Mr. Michael Margulis for his help with the computer graphic work. This work was supported by the Max Planck Society and Deutsche Forschungsgemeinschaft Grant AL549/1-1 (to U.A.) and the Ancell-Teicher Research Foundation for Genetics and Molecular Evolution (to E.N.).

1. Lowrey, L. P. & Takahashi, J. S. (2000) *Annu. Rev. Genet.* **34,** 533–562.
2. Pittendrigh, C. S. (1993) *Annu. Rev. Physiol.* **55,** 15–54.
3. Dunlap, J. C. (1999) *Cell* **96,** 271–290.
4. Hastings, M. & Maywood, E. S. (2000) *BioEssays* **22,** 23–31.
5. Nevo, E. (1991) *Evol. Biol.* **25,** 1–125.
6. Nevo, E. (1999) *Mosaic Evolution of Subterranean Mammals: Regression, Progression, and Global Convergence* (Oxford Univ. Press, Oxford).
7. Nevo, E., Ivanitskaya, E. & Beiles, A. (2001) *Adaptive Radiation of Blind Subterranean Mole Rats* (Backhuys, Leiden).
8. Avivi, A., Albrecht, U., Oster, H., Joel, A., Beiles, A. & Nevo, E. (2001) *Proc. Natl. Acad. Sci. USA* **98,** 13751–13756.
9. Nevo, E. (1998) in *Principles of Animal Design*, eds. Weibel, E. R., Taylor, C. R. & Bolis, C. (Cambridge Univ. Press, Cambridge, U.K.), pp. 288–298.
10. Nevo, E., Guttman, R., Haber, M. & Erez, E. (1982) *J. Mamm.* **63,** 453–463.
11. Tobler, I., Herrmann, M., Cooper, H. M., Negroni, J., Nevo, E. & Achermann, P. (1998) *Behav. Brain Res.* **96,** 173–183.
12. Ben-Shlomo, R., Ritte, U. & Nevo, E. (1995) *Behav. Genet.* **25,** 239–245.
13. Haim, A., Heth, G., Pratt, H. & Nevo, E. (1983) *J. Exp. Biol.* **107,** 59–64.
14. Sanyal, S., Jansen, H. G., de Grip, W. G., Nevo, E. & De Jong, W. W. (1990) *Invest. Ophthalmol. Visual Sci.* **31,** 1398–1404.
15. Pevet, P., Heth, G., Haim, A. & Nevo, E. (1984) *J. Exp. Zool.* **232,** 41–50.
16. Rado, R., Gev, H., Goldman, B. D. & Terkel, J. (1991) in *Photobiology*, ed. Riklis, E. (Plenum, New York), pp. 581–589.
17. Cooper, H. M., Herbin, M. & Nevo, E. (1993) *Nature (London)* **361,** 156–159.
18. Cooper, H. M., Herbin, M. & Nevo, E. (1993) *J. Comp. Neurol.* **328,** 313–350.
19. DeGrip, W. J., Janssen, J. J. M., Foster, R. G., Korf, H. W., Rothschild, K. J., Nevo, E. & de Caluwe, G. L. J. (1992) in *Signal Transduction in Photoreceptor Cells*, eds. Hargrave, P. A., Hofmann, K. P. & Kaupp, U. B. (Springer, Berlin), pp. 43–59.
20. Janssen, J. W. H., Bovee-Geurts, P. H. M., Peeters, Z. P. A., Bowmaker, J. K., Cooper, H. M., David-Gray, Z. K., Nevo, E. & DeGrip, W. J. (2000) *J. Biol. Chem.* **275,** 38674–38679.
21. Argamaso, S. M., Froehlich, A. C., McCall, M. A., Nevo, E., Provencio, I. & Foster, R. G. (1995) *Biophys. Chem.* **56,** 3–11.
22. David-Gray, Z. K., Janssen, J. W. H., Nevo, E. & Foster, R, G. (1998) *Nat. Neurosci.* **12,** 655–656.
23. David-Gray, Z. K., Cooper, H. M., Jannsen, J. W. H., Nevo, E. & Foster, R. G. (1999) *FEBS Lett.* **461,** 343–347.
24. Avivi, A., Joel, A. & Nevo, E. (2001) *Gene* **264,** 45–49.
25. Vuillez, P., Herbin, M., Cooper, H. M., Nevo, E. & Pevet, P. (1994) *Brain Res.* **654,** 81–84.
26. Rehkamper, G., Necker, R. & Nevo, E. (1994) *J. Comp. Neurol.* **347,** 570–584.
27. Frahm, H. D., Rehkamper, G. & Nevo, E. (1997) *J. Brain Res.* **38,** 209–222.
28. Mann, M. D., Rehkamper, G., Reinke, H., Fraham, H. D., Necker, R. & Nevo, E. (1997) *J. Brain Res.* **38,** 47–59.
29. Ben-Shlomo, R., Ritte, U. & Nevo, E. (1996) *Behav. Genet.* **26,** 177–184.
30. Balemans, M. G. M., Pevet, P., Legerstee, W. C. & Nevo, E. (1980) *J. Neural Transm.* **49,** 247–255.
31. Veres, G., Gibbs, R. A., Scherer, S. E. & Caskey, C. T. (1987) *Science* **237,** 415–417.
32. Maniatis, T., Fritsch, E. F. & Sambrook, J. (1982) *Molecular Cloning: A Laboratory Manual* (Cold Spring Harbor Lab. Press, Plainview, NY).
33. Kimura, M. (1983) *The Neutral Theory of Molecular Evolution* (Cambridge Univ. Press, Cambridge, U.K.).
34. Kimura, M. (1980) *J. Mol. Evol.* **16,** 111–120.
35. Li, W. H., Wu, C. I. & Luo, C. C. (1985) *Mol. Biol. Evol.* **2,** 150–174.
36. Li, W. H. (1993) *J. Mol. Evol.* **36,** 96–99.
37. Albrecht, U., Lu, H.-C., Revelli, J.-P., Xu, X.-C., Lotan, R. & Eichele, G. (1998) *Human Genome Methods* (CRC, New York), pp. 93–119
38. Toh, K. L., Jones, C. R., He, Y., Eide, E. J., Hinz, W. A., Virshup, D. M., Ptacek, L. J. & Fu, Y. H. (2001) *Science* **291,** 1040–1043.
39. Albrecht, U., Sun, Z. S., Eichele, G. & Lee, C. C. (1997) *Cell* **91,** 1055–1064.
40. Shearman, L. P., Zylka, M. J., Weaver, D. R., Kolakowski, L. F. & Reppert, S. M. (1997) *Neuron* **19,** 1261–1269.
41. Zylka, M. J., Shearman, L. P., Weaver, D. R. & Reppert, S. M. (1998) *Neuron* **20,** 1103–1110.
42. Liberles, D. A., Schreiber, D. R., Govindarajan, S., Chamberlin, S. G. & Benner, S. A. (2001) *Genome Biol.* **2,** 1–6.
43. Makalowski, W. & Boguski, M. S. (1998) *Proc. Natl. Acad. Sci. USA* **95,** 9407–9412.
44. Gotter, A. L. & Reppert, M. S. (2001) *Mol. Brain Res.* **92,** 19–26.
45. Zheng, B., Larkin, D. W., Albrecht, U., Sun, Z. S., Sage, M., Eichele, G., Lee, C. C. & Bradley, A. (1999) *Nature (London)* **400,** 169–173.
46. Sun, Z. S., Albrecht, U., Zhuchenko, O., Bailey, J., Eichele, G. & Lee, C. C. (1997) *Cell* **90,** 1003–1011.
47. Hogenesch, J. B., Gu, Y. Z., Jain, S. & Bradfield, C. A. (1998) *Proc. Natl. Acad. Sci. USA* **95,** 5474–5479.
48. Bunger, M. K., Wilsbacher, L. D., Moran, S. M., Clendenin, C., Radcliffe, L. A., Hogenesch, J. B., Simon, M. C., Takahashi, J. S. & Bradfield, C. A. (2000) *Cell* **103,** 1009–1017.
49. Schwartz, W. J. & Zimmerman, P. (1990) *J. Neurosci.* **10,** 3685–3694.
50. Albrecht, U., Zheng, B., Larkin, D., Sun, Z. S. & Lee, C. C. (2001) *J. Biol. Rhythms* **16,** 100–104.
51. Shearman, L. P., Jin, X., Lee, C., Reppert, S. M. & Weaver, D. R. (2000) *Mol. Cell. Biol.* **20,** 6269–6275.
52. Bae, K., Jin, X., Maywood, E. S., Hastings, M. H., Reppert, S. M. & Weaver, D. R. (2001) *Neuron* **30,** 525–536.
53. Hardin, P. E. (1994) *Mol. Cell. Biol.* **14,** 7211–7218.
54. Plautz, J. D., Kaneko, M., Hall, J. C. & Kay, S. A. (1997) *Science* **279,** 1632–1635.